07

Study of the influence of current spreading on the operating characteristics of GaP/GaPNAs/GaP micro-LEDs on Si

© L.N. Dvoretckaia[1], A.M. Mozharov[1], V.S. Volosatova[1], V.V. Fedorov[1,2], A.K. Kaveev[1,3], D.V. Miniv[1], I.S. Mukhin[1,2]

[1] Alferov Federal State Budgetary Institution of Higher Education and Science Saint Petersburg National Research Academic University of the Russian Academy of Sciences, St. Petersburg, Russia
[2] Peter the Great Saint-Petersburg Polytechnic University, St. Petersburg, Russia
[3] Ioffe Institute, St. Petersburg, Russia
E-mail: Liliyabutler@gmail.com

Received August 28, 2025
Revised September 23, 2025
Accepted September 24, 2025

A light-emitting semiconductor device based on the GaP/GaPNAs/GaP material system operating in the red-orange spectral range is considered. Numerical modeling of current spreading in the material system under consideration is presented, as well as experimental data demonstrating electroluminescence in the red frequency range. It is shown that for $p-i-n$ GaP/GaPNAs/GaP heterostructures, when forming device light-emitting regions, the creation of separating mesas is not required, since the light emission region is largely limited to the region of the top electrode, which significantly simplifies the technological process of manufacturing LEDs.

Keywords: GaPNAs on Si, GaP on Si, textured GaP(NAs), matrix LED, silicon, semiconductors.

DOI: 10.61011/TPL.2026.02.63029.20485

Bonding of direct-band-gap semiconductor materials and silicon-based electronic components opens up new possibilities for the development of optoelectronic devices in various applications [1,2]. At the same time, direct epitaxy of most direct-band-gap semiconductor A_3B_5 compounds on Si is currently limited by the mismatch of symmetry and crystal lattice constants, which leads to the formation of dislocations and has a negative effect on device operation. In view of this, lattice-matched A_3B_5 substrates (GaAs, InP) are typically used to fabricate optoelectronic elements [3]. Metamorphic thick buffer layers, which make the growth procedure significantly more complicated and, consequently, increase the final cost of heterostructures, are also used [4].

If direct synthesis on Si is not possible, optoelectronic devices on silicon are produced by gluing (bonding) the semiconductor structure to a silicon substrate [5]. A high degree of purity needs to be maintained in the process, since particles with sizes on the order of $1\,\mu$m at the bonding interface have a negative effect on the quality and characteristics of the device as a whole [6,7].

In turn, monolithic epitaxial integration on Si is preferable to the hybrid approach with elements being transferred to the Si surface. Its advantages include scalability, processibility, reduced thermal resistance, and reduced parasitic parameters of electrical interconnections. Depending on the semiconductor material and the device type, optoelectronic devices may be characterized by various parameters, such as wavelength, radiation intensity, structure geometry, etc. For example, high-resolution microdisplays and virtual reality glasses require the fabrication of arrays of micro-emitters or point light sources, which is currently achieved through multi-level technological processing aimed at forming micro-LEDs based on thin-film semiconductor technology [8,9].

The closest lattice matching to silicon is provided by GaP, but this material has an indirect-band-gap structure, which makes it difficult to use in optical structures. In turn, epitaxial GaP heterostructures and its solid solutions (e.g., nitrogen-containing GaP(N,As)) are a new class of semiconductor materials that hold promise for the production of energy-efficient light-emitting diodes operating within the visible and near IR ranges (600−800 nm) [10,11].

The operation of a micro-LED based on a $p-i-n$-GaP(N,As) heterostructure is driven by recombination of electron–hole pairs in the active region of GaPNAs, which leads to the production of photons. Studies into the electro-optical properties of GaPNAs semiconductor heterostructures on Si designed for light-emitting diodes and photovoltaic converters have already been published [12–14]. Optimization of technological processing is required in the context of formation of micro-LEDs on Si with the aim of increasing the resolution of microdisplays operating within the red spectral range.

In the present study, we demonstrate numerically and experimentally that separating mesas are not required when light-emitting device microstructures based on GaP(N,As) are formed on Si, since light emission is largely confined to the top contact due to the low mobility of carriers in emitters. This simplifies significantly the technological process of LED fabrication.

A $p-i-n$ GaP/GaPNAs/GaP heterostructure grown using a Veeco GEN-III setup on a Si substrate by Ni plasma-activated molecular beam epitaxy is considered. Vici-

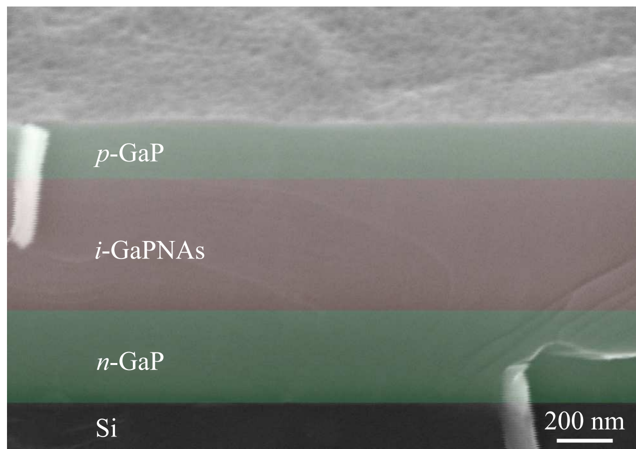

Figure 1. SEM image of a cleaved face of the synthesized $p-i-n$ GaP/GaPNAs/GaP heterostructure and the composition of its layers.

nal (001) silicon substrates with a misorientation angle of $4.0 \pm 0.5^\circ$ in the $\langle 110 \rangle$ direction were used for heterostructure synthesis. These substrates were cleaned by the Shiraki method. Surface silicon oxide was removed by thermal annealing at the minimum required temperature ($T = 820 \pm 10\,^\circ$C, $t = 30$ min). The formation of a uniform Si 2×1 surface reconstruction was observed in the high-energy electron diffraction patterns. Epitaxy of the first GaP buffer layers on Si (001) was carried out in two stages, which ensures the separation of GaP layer nucleation and growth phases. These distinct low-temperature ($450 \pm 10\,^\circ$C) and high-temperature ($580 \pm 10\,^\circ$C) stages provide an opportunity to fabricate an epitaxial layer without twinning. The composition and thickness of layers and the image of a cleaved face of the structure obtained using a scanning electron microscope (SEM) are presented in Fig. 1. To produce a light-emitting device structure, one needs to form ohmic contacts to emitter layers and form device mesas that would constrain the region of injection of carriers and, consequently, their recombination and light emission. Confining mesas are formed by etching a part of the heterostructure in order to constrain the regions of light emission in heterostructures with high carrier mobility (and significant path lengths). Non-radiative recombination centers may emerge in this case on the side wall of a mesa, affecting negatively the LED characteristics. If carrier path lengths are relatively short, the formation of mesas is not required, and emission is confined to the contact region.

The COMSOL Multiphysics numerical simulation package and the AC/DC module were used to study current spreading processes in the GaP/GaPNAs/GaP heterostructure on Si. The examined geometry was comprised of $p-i-n$-structure layers with cross contacts $5\,\mu$m in width formed on opposite sides. This arrangement of contacts ensures that current flows primarily in the region where the electrodes intersect. The discussed geometry is close to a one-dimensional model, but also factors in the finite resistance of emitter layers. To ensure the output of light associated with carrier recombination in the active region, one of the electrodes had a central square hole (window) with sides $1-2\,\mu$m in size. Figure 2 shows the obtained dependences of current spreading in the cross section of the structure.

It can be seen that the flow of current is largely confined to the region of intersection of contacts. The plotted maps allows one to estimate the size of the region of non-uniformity of current density near the intersection of contacts, which was $1.5-2.5\,\mu$m. Thus, it may be concluded that demarcation etching of the heterostructure is not needed to form LEDs if crossed contacts are used, which simplifies the manufacturing process. Analyzing the dimensions of the open window in one of the contacts, we found that the current at the window center drops by 7 % at a window side length of $1\,\mu$m and by 20 % at $2\,\mu$m. Thus, the radiative recombination mechanism in the base will be dominant directly under the metal contact and near the contact, which will lead to an increase in specific conductivity of the base and ensure that a greater part of current flows through it. Owing to the limited lateral conductivity of GaP emitters, this effect will lead to a rapid reduction of potential difference in the emitters distanced laterally from the metal boundary and a transition to the dominant Shockley–Read–Hall recombination mechanism. Thus, the boundary of the region where current non-uniformity (i. e., current spreading) is observed corresponds to the transition from the dominant radiative recombination mechanism to Shockley–Read–Hall recombination. In view of this, perforated electrodes with windows $1-2\,\mu$m in size may be fabricated in order to improve light output.

The process of light output from the active region was simulated numerically for a structure with an active region thickness of 200 nm and an emitter layer thickness of 500 nm. The calculated data for the radiation pattern are presented in Fig. 3. It can be seen that radiation emerging from the structure is largely confined within an opening angle of $\pm 45^\circ$ (relative to the normal to the layer plane). The presence of peaks in the plot is attributable to the formation of standing waves in the thin-film structure and modulation of the light output efficiency. Approximately 30 % of light ultimately overcome the total internal reflection barrier and escape from the structure.

In order to validate the calculated data experimentally, contacts were formed on the grown heterostructure, current–voltage curves were recorded, and the current spreading region in the $p-i-n$-structure was determined. Electroluminescence spectra were also measured.

Laser (Heidelberg DWG 66FS) and projection (Suss MJB4) photolithography was used to fabricate a phototemplate and form a photomask on the heterostructure surface for applying the top contact. Ring Cr/Au (20/150 nm) contact pads were then formed by thermal evaporation of metals in vacuum and lift-off lithography on the surface of the p-GaP emitter layer (Fig. 4, a). The optimum contact formation temperature was $350\,^\circ$C. Aluminum was the

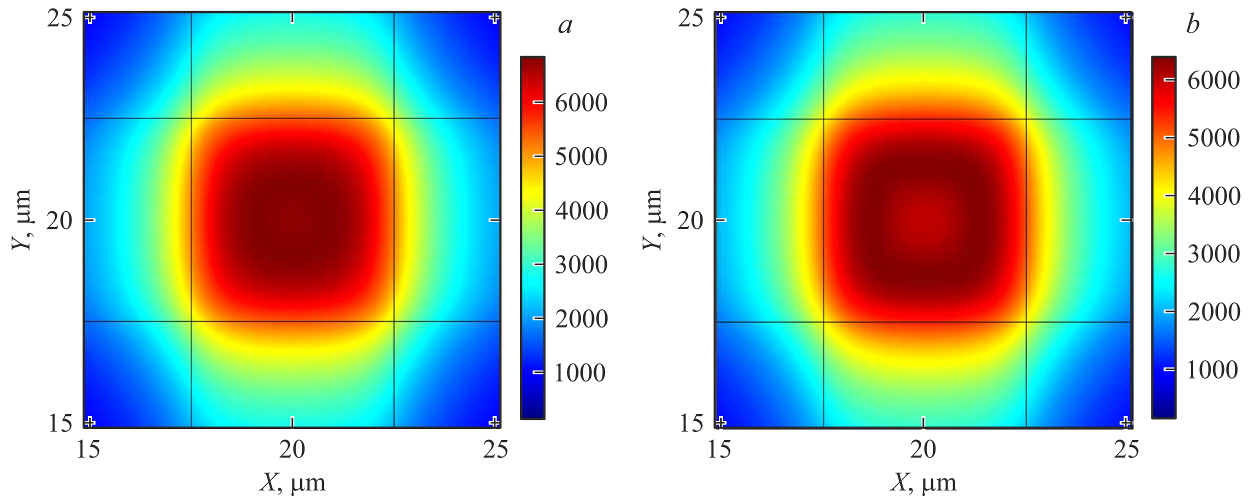

Figure 2. Current spreading maps at an applied bias voltage of 1.8 V for a window 1 (*a*) and 2 μm (*b*) in width.

material of the bottom common contact to the *n*-Si substrate. To negate the effect of surface states on contact with the substrate, the sample was pre-treated in a hydrofluoric acid solution (3:1) for 2 min. This procedure involved removal of the oxide layer from the back surface of the substrate and its hydrogen passivation, which reduced the concentration of surface states sharply for a time sufficient to load the sample into the evaporation system and reach vacuum conditions, thus preventing the formation of a new oxide film.

Measurements revealed electroluminescence of the formed device structures within the red spectral range (Fig. 4, *b*). Examining the optical image of electroluminescence from a single ring (Fig. 4, *c*), one may note the glow along the periphery of the top contact. These results allowed us to estimate the size of the current spreading region at 4–8 μm. The obtained value is of the same order of magnitude as the value determined by numerical modeling, but exceeds it by a factor of 2–4. This deviation is attributable to a certain difference in geometries. In experiments, the doped Si substrate acts as a common electrode, excluding the path of current flow through the bottom emitter layer from the overall size of the spreading region. This raises the conductivity of the emitting structure outside the metal contact by a factor of more than 2 and expands the spreading region by the same amount. The obtained results suggest that the major part of generated light gets lost in the region under the contact and that the geometry of contact layers needs to be optimized in order to ensure efficient radiation output. Specifically, a perforated electrode needs to be fabricated (in accordance with the results of numerical simulation). The recoded current–voltage curve (Fig. 4, *d*) allows us to estimate the opening voltage of the diode structure at 1.8–2 V.

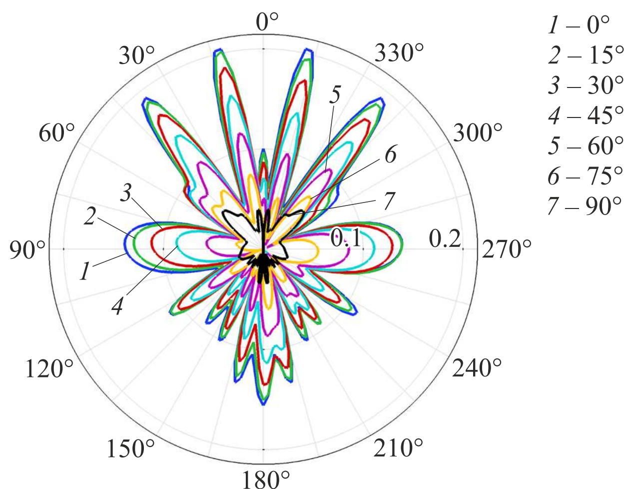

Figure 3. Dependence of the radiation pattern of the LED structure on orientation of a single emitter (dipole).

Thus, numerical modeling of current spreading in a heterostructure revealed that the efficiency of current flow at the center of a window drops by no more than 20 % when square transparent windows with a width of 2 μm in the metallization layer are used. The study of light emission by the structure demonstrated that light is emitted primarily into the solid angle corresponding to a linear angle of 90°.

A high degree of consistency between the results of numerical simulation and experimental data is worthy of note. It was found that the production of device light-emitting regions in the *p*–*i*–*n* GaP/GaPNAs/GaP heterostructure under consideration does not require the formation of separating mesas and that light emission is largely confined to the top electrode region, which simplifies significantly the technological process of LED manufacture. The results of this study bode well for integration with CMOS microcircuits, which will provide a technological basis for the production of advanced microdisplays combining A_3B_5 and Si technologies.

Funding

Experiments were supported financially by grant 23-RB-02-08 from the St. Petersburg Science Foundation.

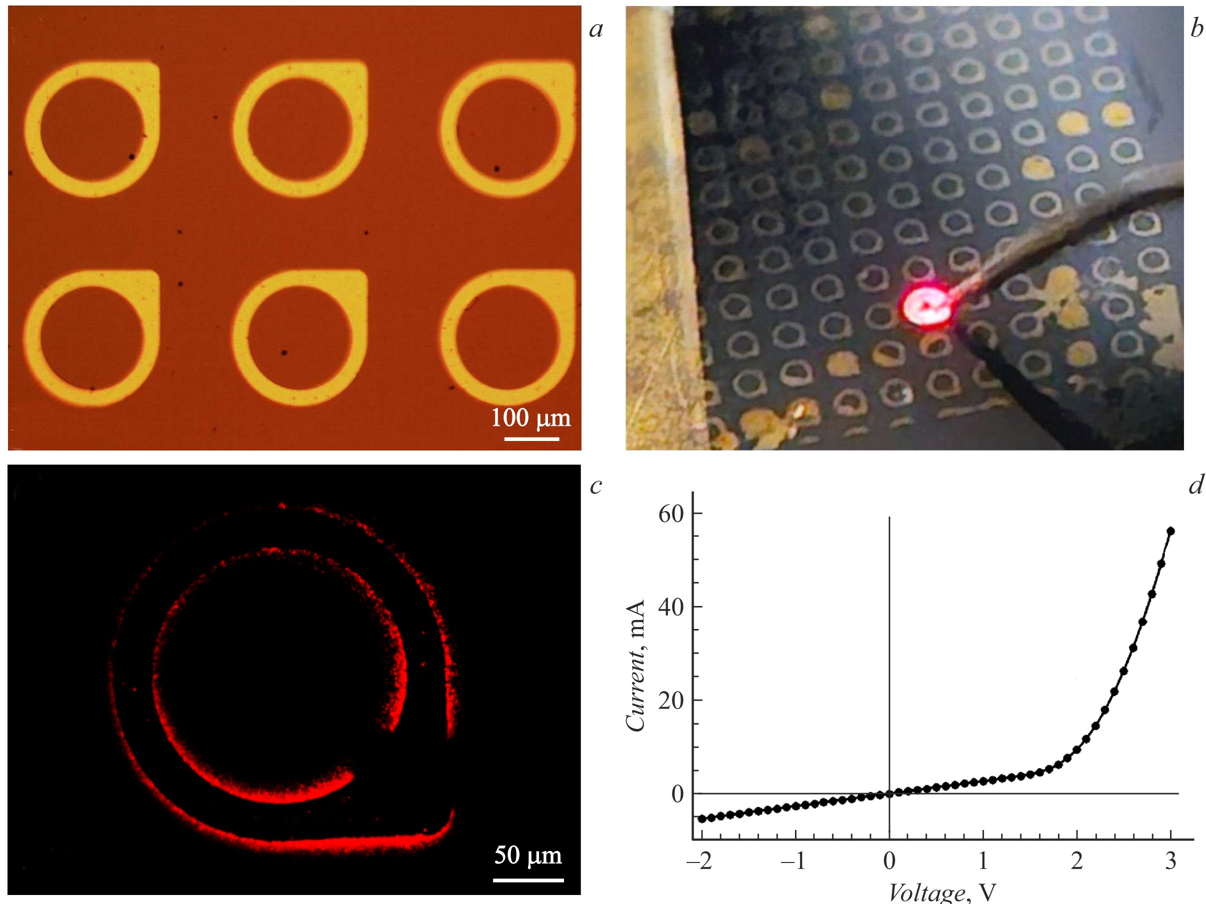

Figure 4. *a* — Optical image of the formed structure; *b* — general view of the experimental sample with an electroluminescent element; *c* — image of electroluminescence from the ring; *d* — typical current–voltage curve.

L.N. Dvoretskaya wishes to thank the Russian Science Foundation (25-72-00195) for financial support of numerical calculations.

Conflict of interest

The authors declare that they have no conflict of interest.

References

[1] G. Roelkens, L. Liu, D. Liang, R. Jones, A. Fang, B. Koch, J. Bowers, Laser Photon. Rev., **6**, 751 (2010). DOI: 10.1002/lpor.200900033

[2] H. Schmid, M.Borg, K. Moselund, L. Gignac, C.M. Breslin, J. Bruley, D. Cutaia, H. Riel, Appl. Phys. Lett., **106** (23), 233101 (2015). DOI: 10.1063/1.4921962

[3] D. Chen, Y.C. Chen, G. Zeng, D.W. Zhang, H.L. Lu, Research, **6**, 0047 (2023). DOI: 10.34133/research.0047

[4] U. Koren, S. Margalit, T. Chen, K. Yu, A. Yariv, N. Bar-Chaim, I. Ury, IEEE J. Quantum Electron., **18** (10), 1653 (1982). DOI: 10.1109/JQE.1982.1071397

[5] F. Zubov, M. Maximov, E. Moiseev, A. Vorobyev, A. Mozharov, Y. Berdnikov, N. Kaluzhnyy, S. Mintairov, M. Kulagina, N. Kryzhanovskaya, A. Zhukov, Opt. Lett., **46** (16), 3853 (2021). DOI: 10.1364/OL.432920

[6] U. Gösele, Q.Y. Tong, Annu. Rev. Mater. Sci., **28** (1), 215 (1998). DOI: 10.1146/annurev.matsci.28.1.215

[7] D. Pasquariello, K. Hjort, IEEE J. Sel. Top. Quantum Electron., **8** (1), 118 (2002). DOI: 10.1109/2944.991407

[8] X. Wu, X. Zhu, S. Wang, X. Tang, T. Lang, V. Belyaev, A. Abduev, A. Kazak, C. Lin, Q. Yan, J. Sun, Materials, **18** (8), 1783 (2025). DOI: 10.3390/ma18081783

[9] J.E. Ryu, S. Park, Y. Park, S.W. Ryu, K. Hwang, H.W. Jang, Adv. Mater., **35** (43), 2204947 (2023). DOI: 10.1002/adma.202204947

[10] R. Kudrawiec, J. Appl. Phys., **105** (6), 063529 (2009). DOI: 10.1063/1.3087781

[11] I.H. Ho, G.B. Stringfellow, J. Cryst. Growth, **178** (1-2), 1 (1997). DOI: 10.1016/S0022-0248(97)00078-X

[12] A.A. Lazarenko, E.V. Nikitina, A.S. Gudovskikh, A.I. Baranov, M.S. Sobolev, E.V. Pirogov, A.Y. Egorov, Opt. Laser Technol., **129**, 106308 (2020). DOI: 10.1016/j.optlastec.2020.106308

[13] A.V. Babichev, V.Yu.Butko, M.S. Sobolev, E.V. Nikitina, N.V. Kryzhanovskaya, A.Yu. Egorov, Semiconductors, **46** (6), 796 (2012). DOI: 10.1134/S106378261206005X.

[14] A.A. Lazarenko, E.V. Nikitina, E.V. Pirogov, A.S. Gudovskikh, A.I. Baranov, A.M. Mizerov, M.S. Sobolev, J. Phys.: Conf. Ser., **2227** (1), 012021 (2022). DOI: 10.1088/1742-6596/2227/1/012021

Translated by D.Safin